

The importance of a correct positioning of the heart using IQ-SPECT system with multifocal collimators in myocardial perfusion imaging: A phantom study

Federico Caobelli, MD, FEBNM,^{a,b} Stefano Ren Kaiser, PhD,^c
James Thomas Thackeray, PhD,^b Frank Michael Bengel, MD, FAHA,^b
Matteo Chierigato, PhD,^c Alberto Soffientini, PhD,^a Claudio Pizzocaro, MD,^a
Giordano Savelli, MD,^a Ugo Paolo Guerra, MD,^a Marco Galelli, PhD,^c and
Orazio Zoccarato, PhD^d

^a Department of Nuclear Medicine, Fondazione Poliambulanza, Brescia, Italy

^b Klinik für Nuklearmedizin, Medizinische Hochschule Hannover, Hannover, Germany

^c Department of Medical Physics, Fondazione Poliambulanza, Brescia, Italy

^d Department of Nuclear Medicine, S. Maugeri Foundation, IRCCS, Scientific Institute of Veruno, Veruno, NO, Italy

Received May 11, 2014; accepted Sep 1, 2014; accepted Sep 2, 2014

doi:10.1007/s12350-014-9994-1

Background. We have recently validated a quarter-time protocol in Myocardial Perfusion Imaging named IQ-SPECT, whose basic principle is to implement a multifocal collimator; However, in clinical practice, it may sometimes be difficult to center the heart in the region of highest magnification of the multifocal collimators (the so-called *sweet spot*). We therefore aimed to evaluate whether a heart mispositioning may affect results in MPI.

Methods. We simulated a rest study with an anthropomorphic phantom with an in vivo distribution of 400 MBq [^{99m}Tc]tetrafosmin, with and without a transmural defect (TD). For each set of images, we performed 5 acquisitions, one with a correct centering and with other 4 degrees of mispositioning. Raw data and reconstructed images were evaluated qualitatively and quantitatively, including no corrections, correction for attenuation, for scatter or for both. We assessed polar plot uniformity, LV wall thickness, and TD and cavity contrast.

Results. Images obtained either with a correct heart centering or with mild mispositioning showed no differences, both qualitatively and quantitatively. Those obtained with major mispositioning differed in uniformity and TD contrast depending on correction parameters.

Conclusion. This is the first study investigating how a heart mispositioning can affect diagnostic accuracy with IQ-SPECT system. Mild-to-moderate mispositioning (≤ 2.5 cm) is unlikely to significantly affect results. (J Nucl Cardiol 2015;22:57–65.)

Key Words: IQ-SPECT • myocardial perfusion imaging • mispositioning • sweet spot • multifocal collimators

The authors disclosure of any personal or financial support or author involvement with organization(s) with financial interest in the subject matter—or any actual or potential conflict of interest.

Reprint requests: Federico Caobelli, MD, FEBNM, Klinik für Nuklearmedizin, Medizinische Hochschule Hannover, Carl Neuberg Straße, 1, 30625, Hannover, Germany; caobelli.federico@mh-hannover.de 1071-3581/\$34.00

Copyright © 2014 American Society of Nuclear Cardiology.

INTRODUCTION

There has been growing interest in recent years directed toward improved systems capable of acquiring myocardial perfusion imaging (MPI) studies at a fraction of time and/or administered dose.

By enhancing the sensitivity of count detection, hardware advances allow for dramatic reduction of acquisition time or tracer doses, thereby contributing to improved patient comfort and lower radiation exposure.¹

Recently, a new system, IQ-SPECT, has been introduced, which was demonstrated in a clinical trial to allow a quarter-time acquisition without loss of diagnostic accuracy.²

IQ-SPECT is based on the implementation of a multifocal collimation, with central focus at the middle of the detector and near-to-parallel focus at the edges, in order to maintain the heart at the most sensitive position of the multifocal collimator (the so-called sweet spot) throughout the entire acquisition. This unique design magnifies the heart, while the edges continue to sample from the whole body, thus avoiding truncation artifacts.³

However, the heart is not automatically positioned at the sweet spot by the IQ-SPECT system; rather, a cursor is manually placed in the center of the left ventricular (LV) cavity by the operator, at which point the two camera heads dynamically adjust to align the heart within the “sweet spot” throughout the entire acquisition.

As a consequence, in clinical practice it may be difficult to center the heart in the “sweet spot” in cases with unclear LV structural anatomy (e.g., with a large perfusion defect), with significant cardiac hypertrophy and wall thinning, with large patient circumference limiting the alignment of the camera heads, or in the case of patient movement. Such cases could negatively impact diagnostic accuracy. We therefore aimed to evaluate the impact of cardiac misalignment with the IQ-SPECT “sweet spot” on image quality and quantitative measurements in MPI in a phantom study.

MATERIALS AND METHODS

Phantom Preparation

We used an anthropomorphic phantom of the chest (Torso Phantom™ and Cardiac Insert™, Data Spectrum Corporation, Hillsborough, NC, USA), with inserts simulating lungs, liver, LV wall, LV chamber, and a removable perfusion transmural defect (TD).

The TD insert (45° × 2 cm) was filled with non-radioactive water and located in mid-to-basal lateral position in the LV wall. The lung inserts, filled with Styrofoam™ beads and non-radioactive water, were used to simulate lung tissue attenuation density.

The other phantom chambers were filled with ^{99m}Tc-solutions at variable radioactivity concentrations (79.5 ± 4 kBq·mL⁻¹ for LV wall, 47 ± 1 kBq·mL⁻¹ for liver, and 3.8 ± 0.2 kBq·mL⁻¹ for chest and LV chamber), in order to simulate an in vivo distribution of 400 MBq, according to data of the literature.^{4,5}

IQ-SPECT System

Images were acquired on a hybrid dual-headed SPECT/CT system (Symbia T, Siemens Medical Solutions AG) equipped with multifocal collimators (Smartzoom™) of 128 × 128 matrix size and zoom factor of 1. Each collimator consists of 48,000 hexagonal holes (1.9 mm diameter, 40 mm length). Spatial resolution is progressively increased from the camera surface to the cardiac “sweet-spot” at 28 cm, which was set as the center of rotation for this study, thereby keeping the LV phantom at the highest magnification throughout the acquisition. A scanning arc of 104° with 6° angular steps was used for each of the camera heads (17 views per detector). Acquired data were then reconstructed using a proprietary iterative reconstruction algorithm (with resolution recovery, 3 iterations, 10 subsets) accounting for gantry deflections, collimator-hole angles, and system point-response function (PRF).² Attenuation correction was applied using a patient-dedicated low-dose CT-derived mu map. An energy-window-based estimate was used to correct for scatter, identifying dual energy windows (127-155 keV primary; 99-126 keV scatter).

Acquisition Protocol

Two sets (i.e., one each with and without TD) of five separate scans were acquired: (1) with the heart centered in the sweet spot (HC), (2) with the left or (3) the right external border centered in the sweet spot (LEB and REB, respectively), thus obtaining a 4.5 cm misposition, and (4) an intermediate misposition to the left (LM), and (5) an intermediate misposition to the right (RM) obtained by centering a point in the sweet spot halfway between the center of the heart and the external borders, thus obtaining a 2-2.5 cm misposition.

Images were analyzed with and without attenuation and/or scatter correction, generating four datasets: non-corrected (NC), attenuation corrected (AC), scatter corrected (SC), and attenuation and scatter corrected (ACSC). The software for SC and AC was provided by the manufacturer using default settings. Alignment between CT and SPECT images was visually verified, but required no user corrections. Images have been qualitatively and quantitatively evaluated.

Visual Analysis

The QPS-QGS software was used to generate polar maps and segment the heart using the 17 segments model. Three experienced readers, blinded to heart positioning and correction information, randomly reviewed the images and evaluated the map uniformity, the extent of TD, and the presence of unexpected artifacts. Interobserver discrepancies were resolved by consensus.

Quantitative Analysis

After reconstruction, all image sets were processed to evaluate the following three measurements associated with image quality in MPI: (1) LV wall thickness; (2) contrast

between LV wall and cavity; (3) contrast between the LV wall and TD.

Wall thickness and LV wall to cavity contrast were evaluated in the image set without the TD insert.

Measurements were performed using ImageJ software⁶ and repeated at least twice by an experienced operator to minimize measurement errors.

LV wall thickness was calculated as “full width at half maximum” (FWHM) of the myocardial signal in the mid-ventricular section of the LV short axis, by fitting the central count profile with a theoretical Gaussian one. The image was summed over three consecutive slices in the mid-ventricular section, and LV wall thickness was estimated as the mean of measurements taken from three different profiles (i.e., anterior, septal, and inferior wall).

Two ROIs were drawn on the mid-ventricular short-axis images for the LV cavity and LV wall in order to estimate the mean counts per voxel for LV wall (η_{LV}) and ventricular chamber (η_{IC}), respectively. The dimensions of the circular ROI drawn on ventricular cavity were kept identical among all acquired images (diameter = 9.6 mm).

Cavity contrast was defined as:

$$\left[\frac{(\eta_{LV} - \eta_{IC}) / (\eta_{LV} + \eta_{IC})}{(C_{LV} - C_{IC}) / (C_{LV} + C_{IC})} \right] \times 100,$$

where C_{LV} and C_{IC} are the true tracer concentrations in the inserts simulating LV wall and left ventricular cavity.

The contrast between TD and LV wall was evaluated in LV short axis by drawing ROIs on the central short-axis images of the phantom acquisitions with TD defect, in order to estimate the mean counts per voxel for the LV wall (η_{LV}) and TD (η_{TD}), respectively. The LV wall ROI was drawn remote from TD location in order to exclude the possibility of counts spilling into the reference region. The dimension of the circular ROI drawn on TD was identical among all acquired images (diameter = 7.6 mm).

TD contrast was defined as:

$$(\eta_{LV} - \eta_{TD}) / \eta_{LV} \times 100.$$

Statistical Analysis

Statistical analysis was performed using SPSS software (version 16.00 for Windows, SPSS Inc., Chicago, IL). All numerical values are given as mean \pm SD. Differences among the acquisitions concerning LV thickness, cavity contrast, TD contrast were assessed by a three-way factorial ANOVA. Correction parameters, positioning combinations, and count statistics were considered as independent variables (factors) and image quality indices as dependent variables. All P values < 0.05 were considered to be statistically significant.

RESULTS

Visual Analysis

All images were scored as of very good quality (Figure 1). In the set of images without TD, there was a

detectable defect in the mid-to-basal infero-lateral wall of left-mispositioned (LM and LEB) images, specifically in images that were not attenuation corrected. The application of attenuation eliminated this defect in LM images and attenuated the defect in LEB images. By contrast, right mispositioned (RM and REB) images displayed a small defect in septal wall in the absence of attenuation correction, which was nearly normalized with AC. In REB images, a small false defect was present in the lateral wall, which was not improved by AC (Figure 2).

The apparent size of TD was enhanced in LM and LEB images when compared to properly centered (HC) images. This apparent increase in TD size was almost normalized by AC. A small persistent apical defect was observed in LEB images, which remained with or without AC. As in the phantom scans without TD, RM and REB images without attenuation correction exhibited a large false defect in septal and, to a lesser extent, inferior wall, which was nearly resolved in attenuation corrected images (Figure 3).

As such, in the absence of AC (i.e., NC and SC images), the inferior wall was more susceptible to attenuation artifacts moving from the left to the right. That is, while the inferior wall showed only a minimal reduction in counts in LEB images, this artifact was more prominent in HC and even more so in REB images. This counts discrepancy was largely resolved in AC and ACSC images.

LV Wall Thickness

The full comparison of wall thickness at multiple scanner positions and image corrections is provided in Table 1. LV wall thickness tended to increase when moving the sweet spot positioning away from the center of the heart toward the right border. This overestimation of the wall thickness was modestly amplified in images without attenuation correction (i.e., NC and SC). However, the differences did not reach a statistical significance ($P = 0.14$) (Figure 4).

Cavity Contrast

Cavity contrast at multiple scanner positions and with various image corrections is provided in Table 2. Contrast tended to be lower in REB images compared to ideal positioning only in AC and ACSC images, though this decrease was not statistically significant ($P = 0.30$). Unsurprisingly, images corrected for attenuation (AC and ACSC) showed an overall higher contrast compared to non-corrected ones (Figure 5).

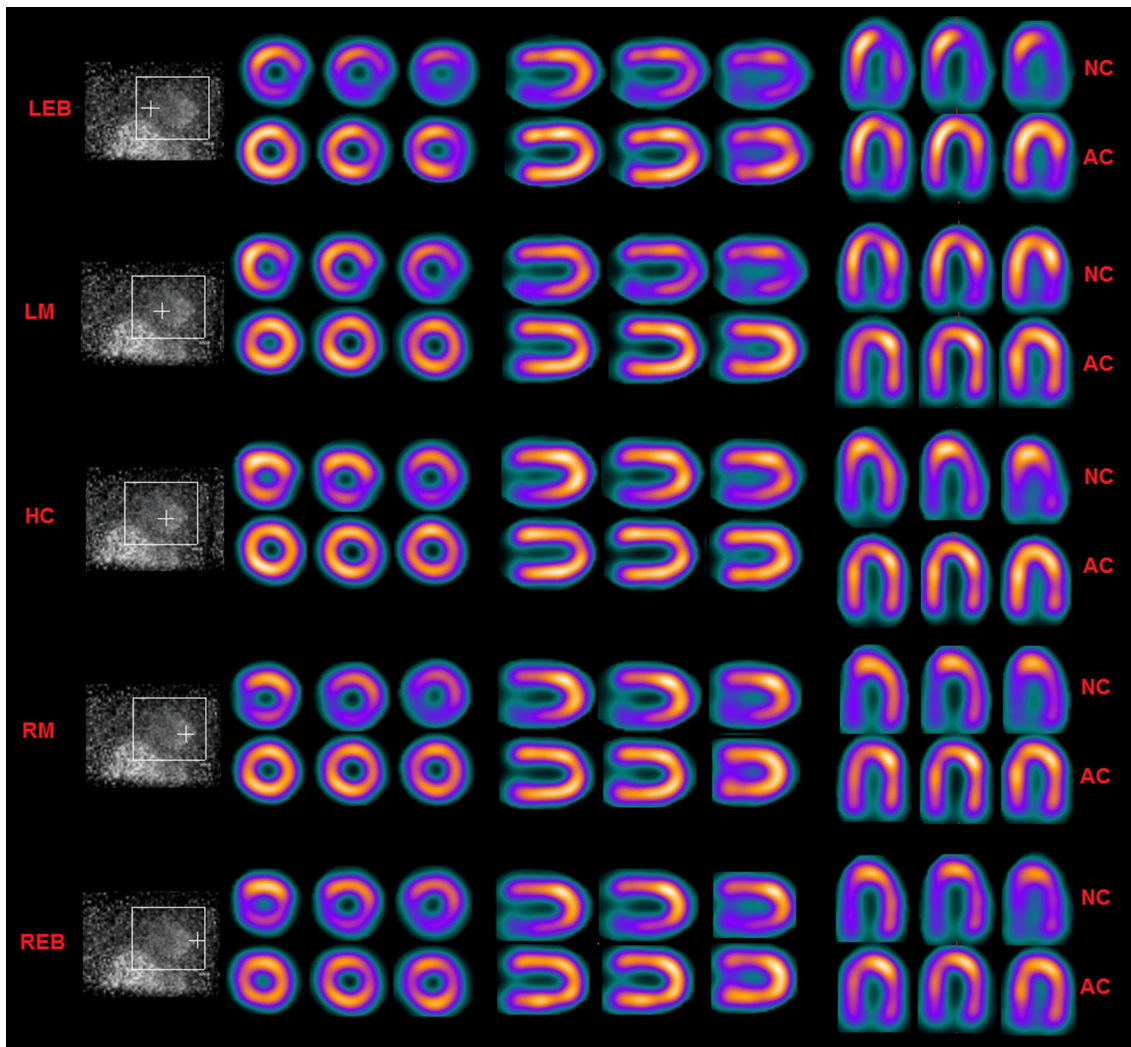


Figure 1. Representative cardiac images (short axis, vertical long axis, horizontal long axis) for each degree of mispositioning. Images refer to the set of images acquired without perfusion defect. The cursor (+) indicates the centering identified by the technologist, by which the system adjusted detector position to maintain the heart within the sweet spot throughout the acquisition.

TD Contrast

TD contrast at multiple scanner positions and with various image corrections is summarized in Table 3. TD contrast depended on the correction applied. In AC and SC images, no differences were observed with either left or right mispositioning. In ACSC images, modestly higher LV wall to TD contrast was noted in left (LEB and LM) or right (REB and RM) mispositioned compared to ideally positioned acquisitions, but these differences were not statistically significant. Finally, in NC images, LV wall to TD contrast was comparable in HC, LM, and RM images, but was significantly and symmetrically decreased in LEB and REB by approximately 35% ($P < 0.05$). As expected, images corrected

for attenuation (AC and ACSC) showed an overall higher contrast (Figure 6).

DISCUSSION

The IQ-SPECT system exhibits advantages in terms of dose reduction, shortening acquisition time,² and improvement in count sensitivity, spatial resolution, and target-to-background ratio.⁷ In particular, the specific geometry of the collimator, with holes focused at the center and near-parallel at the edge, enables enhanced sensitivity for the cardiac region while permitting acquisition of untruncated projection data. In conjunction with a cardiocentric scan orbit at 28 cm to

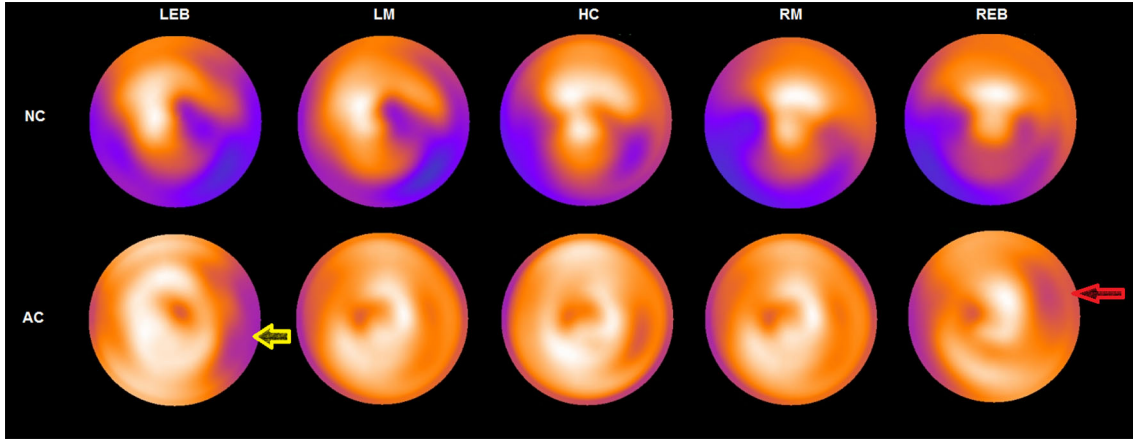


Figure 2. Representative images acquired with a phantom without perfusion defect. Two sets of images are shown as an example, with two different corrections applied (*NC*, upper line, and *AC*, lower line). A detectable defect in mid-to-basal infero-lateral wall in LEB images is present, both with and without attenuation correction (*yellow arrow*). In REB images, a small false defect is visible on attenuation corrected images in the lateral wall (*red arrow*).

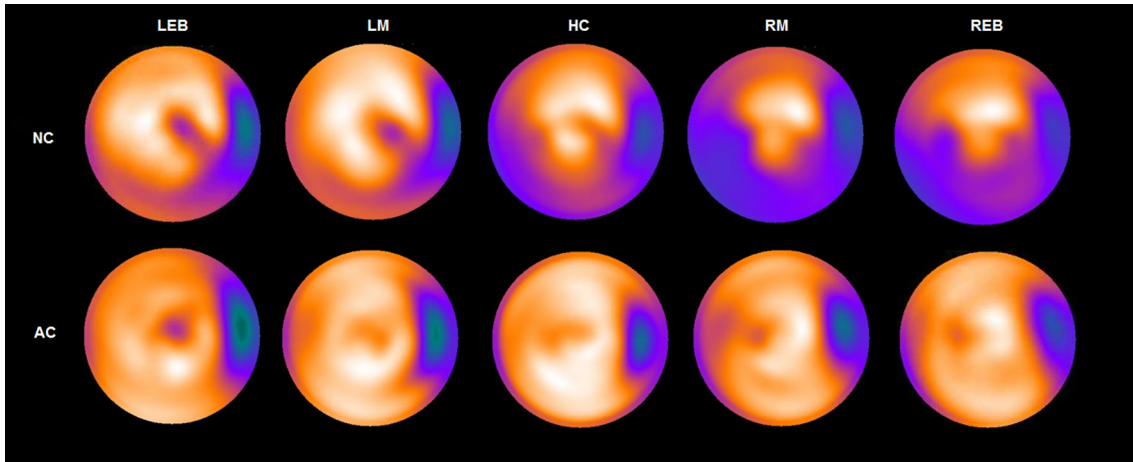


Figure 3. Representative images acquired with a phantom with a simulated transmurial perfusion defect in lateral wall. The same sets of images as in Fig. 2 are shown (*NC*, upper line, and *AC*, lower line). *NC* images show a mild reduction in counts in inferior wall due to attenuation, which becomes to a higher extent moving the centering toward the right border. *AC* images differ only with regard to the extent of TD, being to a higher extent on LEB images.

Table 1. LV wall thickness for different parameters of reconstructions and for different heart positioning

	ACSC		AC		SC		NC	
	FWHM (mm)	SD	FWHM (mm)	SD	FWHM (mm)	SD	FWHM (mm)	SD
LEB	20.9	0.8	21.0	1.1	21.4	1.0	21.2	1.0
LM	21.0	0.8	21.0	0.9	23.5	1.0	23.4	1.0
HC	21.4	0.6	21.8	0.6	24.1	1.0	24.3	0.9
RM	21.5	0.6	22.0	0.6	24.1	1.1	24.1	1.0
REB	22.8	0.8	22.7	0.8	24.3	1.1	23.9	0.9

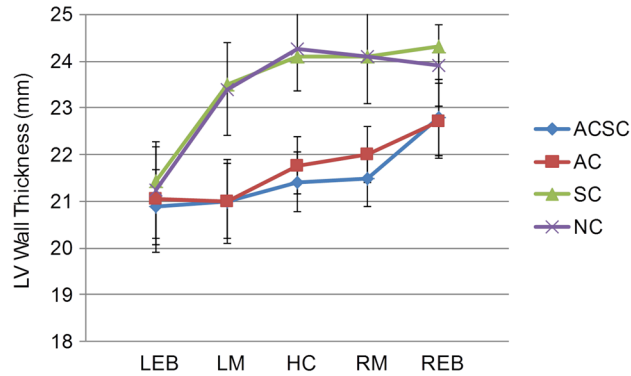


Figure 4. Variability in LV thickness for different heart positions and for different correction parameters. LV thickness tended to be larger moving the heart centering toward the right border, particularly in images not corrected for attenuation. However, differences did not reach a statistical significance. Data are presented as mean \pm SD on a per-pixel basis.

Table 2. Cavity contrast values for different parameters of reconstructions and for different heart positioning

	ACSC		AC		SC		NC	
	Cavity contrast (%)	SD	Cavity contrast (%)	SD	Cavity contrast (%)	SD	Cavity contrast (%)	SD
LEB	94.6	3.8	96.0	2.8	81.3	5.5	84.9	5.2
LM	94.9	3.8	96.0	2.9	82.1	5.3	83.6	5.3
HC	96.5	3.3	96.4	3.4	77.6	4.5	74.5	5.2
RM	95.7	3.2	95.8	3.3	83.9	4.9	83.8	5.2
REB	88.9	4.7	89.3	3.9	83.8	5.0	82.1	5.2

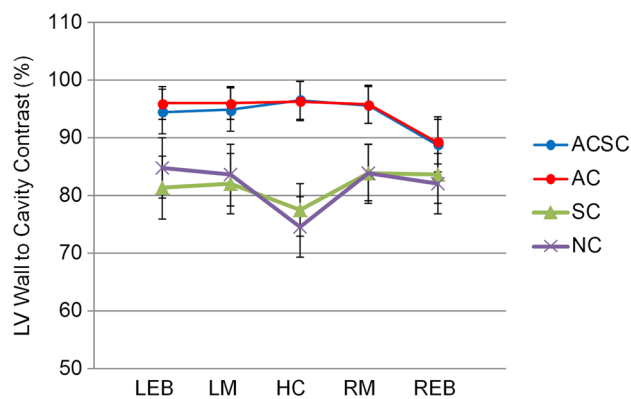


Figure 5. Variability in cavity contrast for different heart positions and for different correction parameters. Differences were not statistically significant, although contrast tended to be lower in images not corrected for attenuation. Data are presented as mean \pm SD on a per-pixel basis.

maximize regional magnification, this configuration provides fourfold higher sensitivity for the cardiac region compared to LEHR parallel-hole collimators.³

However, this unique collimator design requires that the heart be positioned at the point of maximal

magnification, the “sweet-spot”; consequently, a cursor must be manually placed by the operator in the center of the LV cavity to permit the two camera heads to dynamically adjust. This operation may contribute to artifacts and loss of diagnostic accuracy.

Table 3. TD contrast values for different parameters of reconstructions and for different heart positioning

	ACSC		AC		SC		NC	
	TD contrast (%)	SD	TD contrast (%)	SD	TD contrast (%)	SD	TD contrast (%)	SD
LEB	70.2	7.7	70.4	7.0	61.0	7.6	35.8	10.7
LM	74.1	2.3	73.2	3.0	60.7	5.2	65.5	2.7
HC	46.2	3.8	68.2	2.4	55.8	2.5	55.9	2.3
RM	66.9	3.5	65.3	4.4	48.3	5.2	52.3	2.8
REB	52.1	9.5	52.0	9.1	60.7	8.0	35.9	10.9

TD contrast drops in LEB and REB images without corrections (NC) and also in HC images with correction both for attenuation and for scatter

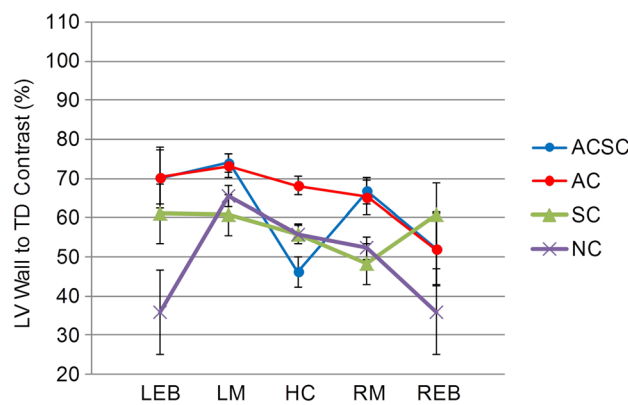


Figure 6. Variability in TD contrast for different heart positions and for different correction parameters. TD contrast was reduced in LEB and REB images without corrections (NC) and also in HC images with corrections both for attenuation and for scatter (ACSC). Data are presented as mean ± SD on a per-pixel basis.

This is the first study investigating the possible effect of heart mispositioning on image outcome using IQ-SPECT. A previous abstract investigated the possible impact on diagnostic accuracy, but was limited to a simulated normal study and only included mild-to-moderate mispositioning (<2 cm),³ whereas our paper investigates the effect of greater mispositioning (up to 4.5 cm) over diagnostic accuracy. Moreover, in the current study, both qualitative and quantitative data were evaluated, as well as investigating the effect upon a simulated abnormal examination, i.e., with a transmural perfusion defect.

From a qualitative point of view, markedly incorrect heart positioning was likely to affect visual interpretation regardless of attenuation or scatter correction. In fact, images from the simulated normal phantom show a persistent false defect in the lateral wall, slightly more prominent on LEB images. Conversely, the effect on interpretation of the TD extent is limited, accounting only for a small difference in apparent size, which was more pronounced with left mispositioning than with

right mispositioning. By contrast, intermediate mispositioning in either direction did not adversely affect qualitative interpretation. Therefore, visual interpretation is unlikely to be affected by mild-to-moderate mispositioning, whereas diagnostic accuracy may be impaired in cases of severe mispositioning.

From a quantitative point of view, no differences in LV wall thickness were identified regardless of mispositioning of the sweet spot or attenuation/scatter correction. However, cavity contrast and, more prominently, TD contrast displayed positioning-dependent abnormalities which were further influenced by the corrections that were performed.

In extreme mispositioning, contrast was decreased considerably, when images were reconstructed without corrections, regardless of right or left misalignment. Intriguingly, TD contrast was lowest with the heart in the correct position, with AC and SC applied, as compared to mispositioned images.

A possible explanation is that an error in scatter measurement can occur, when multifocal collimators are

employed. A recent study by Dong et al. about Cone-beam CT revealed that with different collimator setting the x-ray flat field intensity varies significantly and this can lead to inaccurate scatter measurements. They reported that the large effective focal spot size at low intensities resulted in a great variation of scatter estimation.⁸ Due to the similar geometry of IQ-SPECT collimators, it is likely that a similar incorrect scatter measurement occurs, in which the error is more pronounced, when the heart is centered in the sweet spot. This phenomenon, however, appears to be of particular importance only when SC is associated with AC. We may therefore speculate that the particular collimation shape can influence the estimation of scatter and generation of attenuation maps, particularly with lower counts statistics. The simultaneous application of two correction parameters would amplify such an error and contribute to a degradation of image quality. However, as the differences are not statistically significant, these errors are unlikely to affect diagnostic accuracy.

A recent study investigated the importance of a correct positioning when using cardiac fast cameras,⁹ showing significant increase in SSS and SRS when imaging was performed with the heart outside the center of the normal field of view, compared to optimal positioning.

The authors reported that slight mispositioning (about 5 mm) was sufficient to impair diagnostic accuracy. The present study indicates that only major mispositioning (>2.5 cm) is likely to affect results.

The difference in these results may be explained by different collimator geometry and by the fact that the sweet spot is of sufficient size to include the left ventricle even with mild-to-moderate mispositioning. Additionally, the current results are derived from a phantom study, and therefore, many other variables present in the clinical study⁹ that deviate from the “ideal” model could have affected their results.

Based on the results obtained by applying different corrections, use of AC and NC images appears optimal for IQ-SPECT, whereas SC should be applied with caution, particularly when low doses are administered.

Our study has some limitations. First, acquisitions with different heart positioning were sequentially performed; therefore, results could be theoretically influenced by ^{99m}Tc decay; however, time interval between the first and the last examination was limited (about 20 minutes). Second, these results were obtained in an ideal standard situation and might not be completely applicable in clinical practice, where other confounding factors could affect the results. It should be noted that all acquisitions and data points derive from a single phantom source and activity loading.

We also did not investigate the possible influence of even greater mispositioning. A 4.5 cm misposition is quite severe in standard clinical practice, as in a normal heart, such a misalignment would necessitate a central focus outside of the LV cavity. Moreover, since we have detected differences in image quality at 4.5 cm misposition (i.e., false positive defects), it is probable that greater mispositioning would only amplify this loss of accuracy, and potentially impact quantitative measurements as well. Since we are investigating the best possible conditions on a phantom studies, these discrepancies could be of importance when applied to clinical practice. Finally, the phantom used in this study only allows the evaluation of ungated SPECT images; therefore, the results could be different, when higher counts statistics are required, as in the case of ECG-gated studies, and the impact of motion cannot be evaluated.

Nevertheless, the lack of a significant effect on the quantitative measurements in the phantom study allows for greater confidence in the measurements, regardless of potential mild mispositioning which bears importance for the translation of these results to clinical practice.

NEW KNOWLEDGE GAINED

This is the first paper investigating the effect of heart mispositioning using IQ-SPECT system. Fast camera solutions for MPI have the potential to reduce injected radiation dose but require further validation before implementation into clinical practice. This paper demonstrates that, using the IQ-SPECT system, mild heart mispositioning (≤ 2.5 cm) is likely to be tolerable in clinical practice. This overcomes a potential limit of the system and provides more supportive evidence that this new system can be effectively implemented in clinical practice.

CONCLUSION

In conclusion, mild mispositioning (≤ 2.5 cm) of the heart can be tolerated in IQ-SPECT MPI, and as such is unlikely to adversely affect diagnostic accuracy. Further clinical studies in patients are warranted to validate the clinical relevance of the current findings, especially in patients with potentially complicating conditions such as dilated cardiomyopathy or suboptimal tracer biodistribution.

Ethical Standard

The research reported in the paper was undertaken in compliance with the Helsinki declaration and the International Principles governing research on animals.

References

1. Garcia EV, Faber TL, Esteves FB. Cardiac dedicated ultrafast SPECT cameras: New designs and clinical implications. *J Nucl Med.* 2011;52:210–7.
2. Caobelli F, Pizzocaro C, Paghera B, Guerra UP. Evaluation of patients with coronary artery disease. IQ-SPECT protocol in myocardial perfusion imaging: Preliminary results. *Nuklearmedizin.* 2013;52:178–85.
3. Rajaram R, Bhattacharya M, Ding X, Malmin R, Rempel TD, Vija H, Zeintl J. Tomographic performance characteristics of the IQ-SPECT system. In: *IEEE nuclear science symposium conference record*; 2011.
4. Higley B, Smith FW, Smith T, Gemmell HG, Das Gupta P, Gvozdanovic DV, et al. Technetium-99m-1,2-bis[bis(2-ethoxyethyl)phosphino]ethane: Human biodistribution, dosimetry and safety of a new myocardial perfusion imaging agent. *J Nucl Med.* 1993;34:30–8.
5. Zoccarato O, Scabbio C, De Ponti E, Matheoud R, Leva L, Morzenti S, Menzaghi M, Campini R, Marcassa C, Del Sole A, Garancini S, Crivellaro C, Brambilla M, Lecchi M. Comparative analysis of iterative reconstruction algorithms with resolution recovery for cardiac SPECT studies. A multi-center phantom study. *J Nucl Cardiol.* 2014;21:135–48.
6. Rasband WS. ImageJ. Bethesda, MD: U. S. National Institutes of Health; 1997-2012. <http://imagej.nih.gov/ij/>.
7. Imbert L, Poussier S, Franken PR, Songy B, Verger A, Morel O, Wolf D, Noel A, Karcher G, Marie PY. Compared performance of high-sensitivity cameras dedicated to myocardial perfusion SPECT: A comprehensive analysis of phantom and human images. *J Nucl Med.* 2012;53:1897–903.
8. Dong X, Niu T, Jia X, Zhu L. Relationship between X-ray illumination field size and flat field intensity and its impacts on X-ray imaging. *Med Phys.* 2012;39:5901–9.
9. Hindorf C, Oddstig J, Hedeer F, Hansson MJ, Jögi J, Engblom H. Importance of correct patient positioning in myocardial perfusion SPECT when using a CZT camera. *J Nucl Cardiol.* 2014;21:695–702.